ELSEVIER

Journal of Molecular Catalysis A: Chemical 171 (2001) 181–190

JOURNAL OF MOLECULAR CATALYSIS A: CHEMICAL

www.elsevier.com/locate/molcata

The influence of Fe on the dispersion, electronic state, sulfur-resistance and catalysis of platinum supported on KL zeolite

J. Zheng [a,1], T. Schmauke [a], E. Roduner [a,*], J.L. Dong [b], Q.H. Xu [b]

[a] *Institute of Physical Chemistry, University of Stuttgart, Pfaffenwaldring 55, 70569 Stuttgart, Germany*
[b] *Department of Chemistry, Nanjing University, Nanjing 210093, PR China*

Received 19 September 2000; received in revised form 14 November 2000; accepted 6 February 2001

Abstract

The influence of Fe as a second metal component on the decomposition, dispersion and catalysis of the platinum amine complex in KL zeolite has been investigated. TG-DTA was used to measure the decomposition of the complex in KL and Fe/KL zeolites. XPS showed that Pt^{2+} and in particular Fe^{3+} ions show strong surface enrichment after calcination. Partial reduction of Fe^{3+} was found to occur both under calcination (autoreduction) and reduction (in a hydrogen atmosphere) treatments, as evidenced by an increase of the ESR signal at $g = 2.3$. Both, ESR and TPR results revealed that platinum catalyzes the reduction of Fe^{3+}, leading to a nearly 100 K decrease of the reduction temperature. Bimetallic Pt–Fe particles were thus produced, exhibiting better dispersion than mono-metallic Pt/KL zeolite, as determined by TEM. The catalytic properties of Pt–Fe/KL zeolite varied with the amount of Fe. At 0.3 wt.% Fe, the catalyst was found to show both excellent *n*-hexane aromatization reactivity and higher sulfur-resistance. An interpretation of the differences in the catalytic performance based on the particle size and electronic state of active platinum by Pt–Fe interaction is discussed.

Keywords: Pt–Fe/KL zeolite; *N*-hexane aromatization; Sulfur-resistance

1. Introduction

The preparation of highly dispersed Pt on zeolites has become the focus of many studies [1–5]. It has been demonstrated that the dispersion of Pt/zeolite is strictly related to the preparation history, in particular, to the temperature of calcination and reduction [2]. A clear trend of increasing catalytic activities with decreasing Pt cluster size has also been found [3].

Sachtler and coworkers have investigated methods to achieve and maintain a high dispersion of Pt metals. They found that less reducible transition metal cations (such as Fe^{2+} ions) introduced into Pt/NaY stabilize Pt^{2+} ions during and/or after calcination and act as "chemical anchors" for the platinum particles after reduction. This favors a high dispersion of platinum [2,5].

Bimetallic catalysts are of increasing importance due to the promoting action that second components can have on the activity and/or selectivity of a particular catalytic metal, mainly by virtue of alloy formation [6]. Many state of the art industrial catalysts are complicated mixtures of at least two metals plus one or several dopants, such as the conventional bifunctional reforming catalyst ($Pt–Re/Al_2O_3–Cl$).

* Corresponding author. Tel.: +49-711-685-4490; fax: +49-711-685-4495.
E-mail address: e.roduner@ipc.uni-stuttgart.de (E. Roduner).
[1] Present address: Applied Catalysis in Energy Laboratory, Pennsylvania State University, 209 Academic Projects Building, University Park, PA 16802-2303, USA.

1381-1169/01/$ – see front matter
PII: S1381-1169(01)00096-6

Usually, the two highly dispersed catalytic components in a bimetallic catalyst are considered to exist as an alloy or as bimetallic clusters. However, evidence has also been found that only one of the components is in the metallic state, while the other one remains in an oxidized state after reduction [7–10]. For the cases of Rh–Fe/NaY and Pd–Fe/NaY, direct evidence was presented that part of the iron is reduced to Fe^0 and that this portion is alloyed to the other metal, while the remaining iron is reduced from Fe^{3+} to Fe^{2+}. In the case of monometalic Fe zeolites the reduction to Fe^0 is not possible. TPR and TPD experiments indicate that 5% of the iron in Pd–Fe/NaHY and 15% in neutralized Pd–Fe/NaY are present as Fe^0, and all detectable palladium is alloyed to Fe and thus unable to form beta-Pd-hydride which is typical for monometalic Pd/NaY catalysts [8]. For Rh–Fe/NaY systems the amount of Fe^0 ranged between 3 and 100%, depending on the preparation conditions [9,10]. By ferromagnetic resonance a broad and intense signal is detected in the case of Rh–Fe systems but not in monometalic Fe zeolites. It can certainly be attributed either to metallic iron or to PdFe alloy [8,10]. Mössbauer spectroscopy indicates as well that part of the iron is reduced to Fe^0, although this is still a matter of debate [8–10]. It is, therefore, vital to characterize the state of the bimetallic components and to establish what factors influence the relationship between the metals during catalyst preparation.

Pt supported on KL zeolite, specifically, was found to be a highly active and selective catalyst for the aromatization of *n*-hexane, the selectivity to benzene being six to eight times higher than that of the conventional bifunctional reforming catalyst (Pt–Re/Al_2O_3–Cl) [11]. Although still under debate, it is mainly accepted that the non-acidic channel structure is important for the very high dispersion of Pt particles which are the only active sites for the aromatization of *n*-hexane in this catalyst [12–14]. Any acidity introduced during preparation may decrease the selectivity [15].

However, a mono-functional Pt/KL catalyst showed much higher sensitivity to sulfur poisoning than the conventional catalyst. This prevented its application in industry to higher extent [16]. Several mechanisms have been put forward to explain the phenomenon. Vaarkamp et al. [17] and McViker et al. [18] arrived at the same conclusion that the high sensitivity to sulfur poisoning of Pt/LTL could be attributed to the loss of active platinum surface by adsorption of sulfur and to the growth of Pt clusters, whereas Fukunaga and Ponec suggested that K^+ in a Pt/KL catalyst could be responsible for both the high aromatization activity and the high sulfur sensitivity [19].

According to literature, the way to alter the intrinsic sulfur-resistance of a metal is through a modification of its electronic properties. Catalysts containing electron-deficient metal atoms on the surface are more resistant to sulfur poisoning than those containing metal atoms with a higher electron density [20]. Electron-deficient species can be formed either by interaction of the metal with acid sites on the support [21], by changing the metallic particle size to get nearly atomic dispersion [1], or by bimetallic interaction [22,23].

There is general agreement that a noble metal is more sulfur tolerant on acidic supports than on non-acidic supports [20]. However, this way of improving the sulfur resistance is not very acceptable here since it is not favorable to a Pt/L catalyst for *n*-hexane aromatization as mentioned above. Alternatively, cations with a high valence state can act as electron-acceptor sites and improve the sulfur resistance of Pt due to their Lewis acid character [24].

Introduction of other metal components such as Re and W [25], Fe [26], and rare earths (La and Dy) [27] has also been studied, but few of them can improve both the aromatization reactivity and the sulfur-resistance of a Pt/KL catalyst.

In this paper, we investigate the influence of a co-impregnated second metal component (Fe) on the decomposition, dispersion and catalysis of the platinum amine complex in KL zeolite. DTA and TEM were used to study the location and dispersion of Pt particles with iron incorporation, hexane pulse-flow micro-reaction to investigate the catalytic reactivity and sulfur-resistance. The interaction between platinum and iron, evidenced by TPR and ESR, was used to explain the different catalytic performance.

2. Experimental

2.1. Sample preparation

KL zeolite was obtained as described previously (with Si/Al = 3.2) [28] and also from CU Chemie

Uetikon AG (Si/Al = 3.0), both having standard LTL structure. Incipient wetness impregnation of $Pt(NH_3)_2Cl_2$ (*cis*-platinum, Aldrich Chem Co.) was performed at 353 K, and yielded Pt/KL samples of 0.6, 1, and 5 wt.% platinum loading, respectively. In the case of bimetallic Pt–Fe/KL samples, $Fe(NO_3)_3{\cdot}9H_2O$ (Aldrich) and $Pt(NH_3)_2Cl_2$ were co-impregnated. The samples were then dried at 383 K for 1 h and kept in a desiccator.

As-synthesized samples were calcined in a high flow of O_2 (200 ml/min) in a packed bed reactor. The temperature was raised at 0.5 K/min from room temperature to 573 K where it was kept for 1 h.

2.2. Characterization

Gravimetric-differential thermal analysis (TG-DTA) studies were carried out under air using a Rigaku TG-DTA instrument with uncalcined mono- and/or bi-metallic Pt containing samples of about 30 mg. The temperature was raised at 20 K/min from room temperature to 1173 K. A broad instrumental background independent of samples was observed.

The binding energy and surface composition of Pt and Fe species on calcined samples were determined using X-ray photo-spectroscopy (XPS), obtained by an ESCALAB MK instrument with Mg–K X-ray. The binding energies were referenced to the C_{1s} line at 285.0 eV. The ratio of atomic concentration on the surface layer designated as (Si/M)s was estimated from the XPS peak area of the $Pt_{4d5/2}$, Al_{2s}, Si_{2p} and Fe_{2p} lines.

Temperature programmed reduction (TPR) experiments were performed on calcined samples (50 mg) in 5.5% H_2/N_2 atmosphere (30 ml/min) while the temperature was increased to 873 K at a heating rate of 8 K/min. A 5 A molecular sieve was used in front of the TCD detector to remove H_2O and NH_3 formed during reduction.

The metal particle size distribution of the reduced samples was determined by transmittance electron micropscopy (TEM) using an EM 400 instrument with a magnification of 175,000, by evaluating more than 300 particles.

Fourier-transform infrared spectroscopy (FTIR, on a Nicolet 510P instrument) on adsorbed CO was carried out at room temperature using self-supported zeolite wafers (8 mg/cm^2). After reduction in H_2, the samples were dehydrated at 623 K for 2 h. CO gas was admitted at a pressure of 4×10^4 Pa followed by evacuation.

Electron spin resonance (ESR) was used to obtain information mainly on iron species. After every treatment, the same amount of sample was transferred from the packed bed reactor to an ESR tube in a glove box, followed by evacuation overnight at room temperature. For reduction, samples were heated in flowing H_2 (30 ml/min) with a ramping rate of 8 K/min, and kept at the final temperature for 1 h. X-band ESR spectra were recorded on a Bruker EMX spectrometer in a temperature range 4–296 K. Bruker software was used for double integration. To compare different ESR spectra, the acquisition parameters were kept constant, and the microwave power was maintained below the saturation level.

2.3. Catalytic studies

As-synthesized Pt/KL or Pt–Fe/KL catalyst was pelleted and screened through 20–40 mesh. In each run, 50 mg catalyst on a dry basis was placed in a pulse flow micro-reactor. All catalysts were calcined and then reduced with hydrogen at 773 K for 2 h. 3.1 mol of hexane was injected to the reactor at 773 K with hydrogen as carrier gas (30 ml/min). In order to study sulfur poisoning, hexane containing 0.2 ppm thiophene was injected instead of pure hexane. The reaction products were analyzed by on-line gas chromatography with a thermal conductivity detector and DNP columns (di-*n*-nonyl phthalate).

3. Results and discussion

3.1. Reactivity and sulfur-poisoning of the catalysts

The lowest amount of Pt necessary to achieve high catalytic performance in KL zeolite was found by us previously to be 0.6 wt.%. A higher loading does not increase significantly the aromatization selectivity [29]. From an economic point of view, the amount of Pt for the catalysis was therefore chosen to be as small as possible (0.6 wt.%). Fig. 1 shows the *n*-hexane (a) and sulfur containing *n*-hexane (b) aromatization reactivity of 0.6% Pt supported KL catalyst as a function

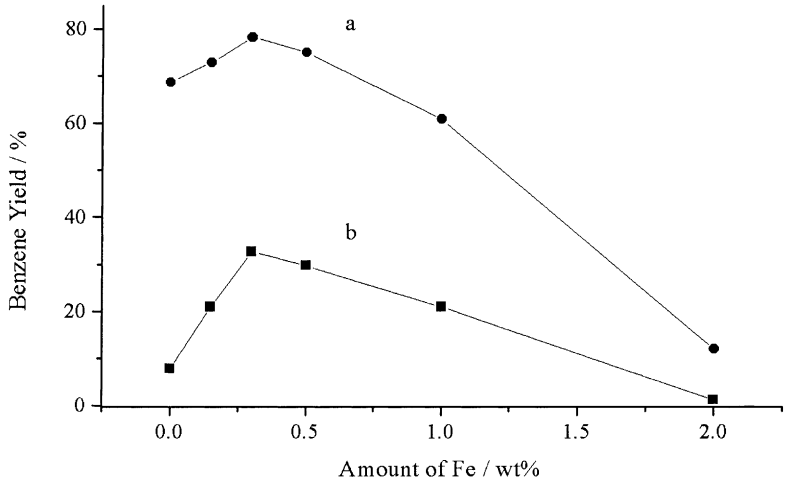

Fig. 1. (a) *n*-Hexane and (b) *n*-hexane containing 0.2 ppm thiophene aromatization reactivity of Pt–Fe/KL as a function of the amount of Fe at 773 K.

of Fe content. A doping level of 0.3 wt.% of Fe shows to be the most effective for *n*-hexane aromatization.

Sulfur is known to be a severe poison of metal catalysts because sulfur compounds are strongly chemisorbed on the metal surface [28]. Fig. 1 confirms this for the present case since the benzene yield drops greatly when the reactant contains only a trace amount of sulfur (curve b). Nevertheless, a proper iron content (0.3 wt.%) improves somewhat the sulfur resistance of the Pt supported KL zeolite.

In order to study the process of sulfur poisoning in more detail, *n*-hexane containing 0.2 ppm thiophene was used as reactant for different length of time in the pulse-flow micro-reactor. Fig. 2 shows again that Pt/KL is very sensitive to sulfur poisoning: after six reactant pulses it loses its reactivity to benzene almost completely (curve b), whereas the 0.6% Pt-0.3% Fe/KL bimetallic zeolite shows a significantly higher resistance to sulfur poisoning (curve c), with a remaining benzene yield of 40% after six pulses.

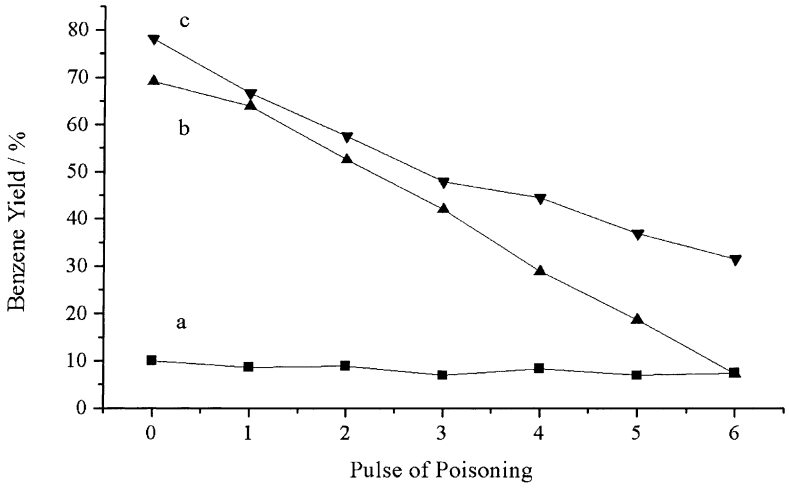

Fig. 2. Sulfur poisoning curves at 773 K for (a) Pt–Re/Al_2O_3–Cl; (b) 0.6% Pt/KL; (c) 0.6% Pt-0.3% Fe/KL.

Table 1
Results of TEM and CO-IR

Samples	Fe (wt.%)	d (nm)	$\%d <$ 2.5 nm	ν_{CO} (cm^{-1})
Pt/KL	0	2.4	68	2035
Pt–Fe/KL-1	0.15	1.9	91	–
Pt–Fe/KL-2	0.3	2.1	83	2054
Pt–Fe/KL-3	1.0	3.3	16	–

The industrial catalyst (Pt–Re/Al_2O_3–Cl) shows very high sulfur resistance, but the catalytic activity is too low (Fig. 2, curve a). It is clear that a 0.6% Pt-0.3% Fe/KL bimetallic zeolite is superior than the mono-metallic Pt/KL and the conventional catalyst. It is our intention to understand why a proper amount of iron improves both the aromatization catalysis and the sulfur resistance of the Pt/KL catalyst.

3.2. Dispersion and electronic state of Pt particles after reduction

Table 1 gives the distribution of Pt particle size on the reduced samples based on the TEM determination (pictures not shown). Most Pt particles in 0.6% Pt-0.3% Fe/KL zeolite are in the range of 1–2.5 nm, which were believed to be the most active for *n*-hexane aromatization [30]. No very large particles could be found in this sample. The average size in the bimetallic sample is 2.1 nm, and the fraction of particles smaller than 2.5 nm is 83%, showing somewhat higher Pt dispersion than that of 0.6% Pt/KL zeolite with an average Pt particle size of 2.4 nm and a fraction of 68% of particles smaller than 2.5 nm. This confirms that the proper amount of incorporated iron is favorable for a higher Pt dispersion. However, when the amount of Fe increases to 1.0 wt.%, the dispersion decreases. Combining the result of TEM with the catalysis (as seen in Fig. 1), we find a rough trend of increasing *n*-hexane aromatization reactivity with decreasing Pt particle size, which confirms our earlier observations [3].

Infrared spectroscopy of adsorbed CO is frequently used as a method to determine the electronic state and also particle size effect of Pt metal supported on zeolites [3,31]. On Pt/KL we observe CO at 2035 cm^{-1} (Table 1), which is attributed to linearly bound CO on Pt [32]. A shift of this band to 2054 cm^{-1} on Pt–Fe/KL shows that Fe makes the Pt particles more electron-deficient.

The resistance to sulfur poisoning is suggested to arise from the smaller binding energy of electronegative sulfur atoms on electron-deficient Pt clusters [20]. The nature of the interaction of Fe which renders Pt more electrophilic is the main objective of the work described below. To this end, it is important to understand what happens during sample preparation, mainly calcination and reduction.

3.3. Decomposition of the platinum amine complex and migration of Pt^{2+} ions

TG-DTA is a rapid and direct method to study the thermal decomposition of compounds. Owing to the limiting sensitivity, the amount of Pt was increased to 5 wt.%. Fig. 3 shows TG-DTA results of plain KL zeolite (a), as-synthesized 5% Pt/KL (b), and 5% Pt-0.3% Fe/KL (c). The small endothermic DTA peaks around 373 K in plain KL, accompanied by major weight loss

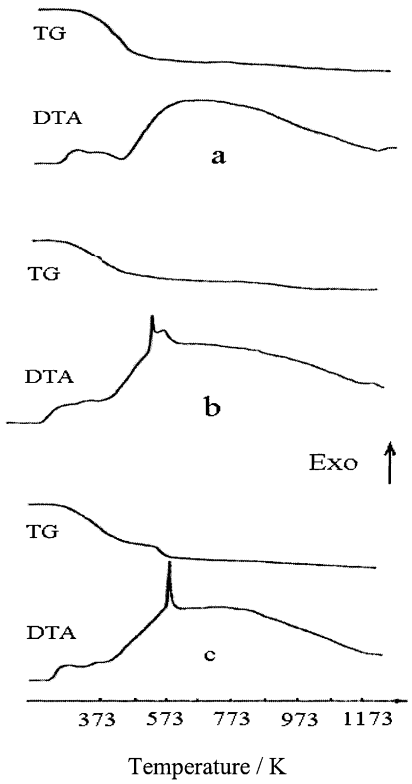

Fig. 3. TG-DTA results of (a) plain KL zeolite, and as-synthesized (b) 5% Pt/KL; (c) 5% Pt-0.3% Fe/KL.

Table 2
XPS results of samples after calcination at 573 K

Samples	BE (eV)		Experimental (nominal) atomic ratios			
	$Pt_{4d5/2}$	Fe_{2p}	Si/Al	Pt/Al	Fe/Al	Pt/Fe
5% Pt/KL	315.7	–	2.6 (3.1)	0.16 (0.080)	–	–
5% Pt-0.3% Fe/KL	315.7	709.8	2.6 (3.1)	0.13 (0.080)	0.33 (0.017)	0.39 (4.8)
0.3% Fe/KL	–	709.8	2.5 (3.2)	–	0.67 (0.018)	–

in TG curves, are due to the desorption of physically adsorbed water. During the further increase of temperature, a broad DTA curve is found on all samples including plain KL zeolite itself, which is therefore not related to the decomposition of the platinum complex.

The sharp exothermic DTA peaks at about 548 and 576 K are attributed to the decomposition of *cis*-$Pt(NH_3)_2Cl_2$ dispersed in different locations in KL. Previously, we studied the decomposition of the same complex supported on β zeolite [33]. A series of three exothermic DTA peaks was found at 558, 596 and 634 K, respectively, whereas *cis*-platinum itself shows one sharp "explosive" peak at 583 K [33]. Combined with the present study this is clear evidence of the effect of zeolite structure and of the site in the zeolite where the complex is located. Generally speaking, a platinum complex stabilized in more hidden sites of a zeolite channel needs higher decomposition temperature.

It is interesting to find that two DTA peaks appear in mono Pt/KL sample (curve b), while only one peak at higher temperature appears in the bimetallic one (curve c). This indicates that iron co-impregnation stabilizes the platinum complexes.

XPS has been extensively used to study the oxidation state of noble metals in zeolites [34]. It is sensitive to a range of about 5 nm from the crystal surface. Since the peak belonging to Pt_{4f} is seriously overlapped by the peak of Al_{2p}, the broad $Pt_{4d5/2}$ peak has to be used as an indicator of the state of Pt. The results are given in Table 2, together with the nominal ratios based on the bulk composition. It is found that the binding energies of Pt and Fe (Fe_{2p}) in 5% Pt-0.3% Fe/KL are the same as for the mono-metallic zeolite, showing the same electronic states of Pt (Pt^{2+}) and Fe (Fe^{3+}) in KL after calcination within the experimental limitation of XPS.

Inspection of Table 2 shows that the experimental Si/Al ratio is slightly below the nominal value based on the bulk composition, indicating a slight enrichment of Al at the surface as it has been found in other cases. Surface enrichment of Pt amounts to a factor of 2 based on Pt/Al and is thus more significant, but it is particularly spectacular for Fe, reaching a factor of 20–40 based on Fe/Al. Upon calcination, Pt^{2+} and Fe^{3+} ions lose their ligands (NH_3, Cl^-, H_2O/OH^-) and migrate onto the inner surface to coordinate with the zeolite framework. The large surface enrichment of Fe demonstrates the superiority of Pt^{2+} ions in the extent of migration. While these experiments give us the situation after calcination, it would be of interest also to know what it is after reduction. Considering that any reduced sample would unavoidably be re-exposed to air during XPS measurements at the available instrument, we did not carry out XPS experiments on reduced samples. The above CO-FTIR measurements after reduction indicate that all the Pt that is accessible to CO is influenced by Fe. The problem will be further discussed in Section 3.4. A pronounced outer surface enrichment of Fe has also been reported by Bartholomew and Boudart on the system of Pt–Fe alloy supported carbon [35].

The Fe/Al and Pt/Al ratios of the bimetallic sample are somewhat smaller than those of the mono-metallic samples. This may indicate a correlation of the migration of Pt^{2+} and Fe^{3+} ions onto the inner surface of the zeolite.

The high sensitivity of the ESR technique for the characterization of iron species can give us more information than conventional methods. Fig. 4 shows the room temperature ESR spectra of the samples after calcination. KL zeolite (Fig. 4a) itself shows ESR signals attributed to Fe^{3+} impurities in the zeolite as discussed in detail in literature [36,37]. The X-band

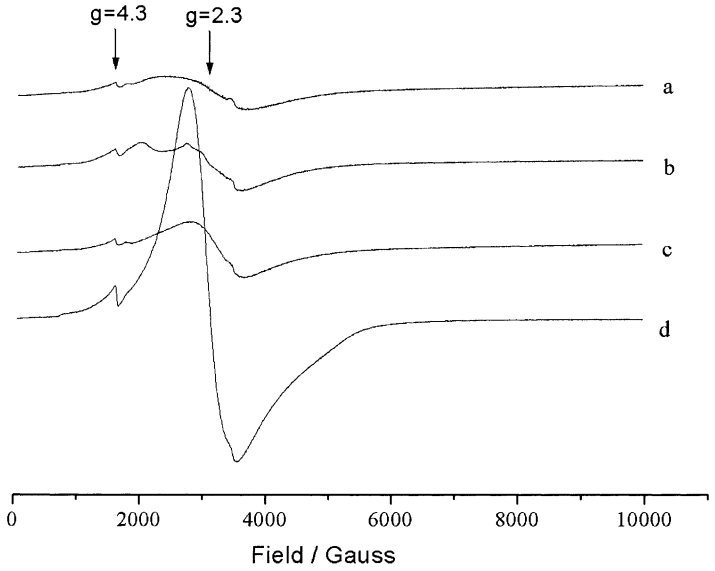

Fig. 4. Room temperature ESR spectra of samples after calcination: (a) KL; (b) 5% Pt/KL; (c) 0.3% Fe/KL; (d) 5% Pt-0.3% Fe/KL.

ESR spectrum usually consists of three major signals at $g = 4.3$, 2.2–2.3, and 2.0. The commonly accepted assignment, although still under debate [37], has been as follows: framework iron, iron in interstitial oxide or hydroxide phases, and iron in cation-exchange sites, respectively. In our samples, there are usually two ESR signals at $g = 4.3$ and 2.3. When additional iron was introduced as in the 0.3% Fe/KL sample (Fig. 4c, comparing with Fig. 4a), there is a slight increase in the intensity of the signal with a g factor around 2.3. This signal is our main concern since the additional iron was introduced by impregnation, which usually does not permit framework substitution.

It is interesting to find that, in contrast to the mono-iron supported zeolite, there is a large increase of the $g = 2.3$ signal in the bimetallic Pt–Fe/KL zeolite after calcination treatment (Fig. 4d). As already pointed out by others, this could be due to partial reduction of Fe^{3+} to Fe^{2+} (or Fe^{0}) [38–40]. With exceptions, Fe^{2+} ions are not active in X-band ESR and measurements at temperatures of $T > 4$ K. However, if Fe^{2+} is combined with Fe^{3+}, a very strong and broad signal is observed [38]. This is ascribed to a change of the magnetic properties of the iron oxide/hydroxide clusters, for example by a partial release of the near-complete cancellation of spins of antiferromagnetically coupled ions. Also, ferromagnetic iron in the reduced state was found to display a large ESR spin intensity [39]. Therefore, our ESR results indicate that partial reduction of Fe^{3+} occurred during calcination of bimetallic samples even in oxidative atmosphere. This may be explained as follows.

During calcination, the NH_3 ligands of the *cis*-platinum are removed from the Pt^{2+} ions, and they can bind to any Lewis acidic site in the zeolite and then reduce ions like Pt^{2+} or Fe^{3+} species. Previously we have studied the autoreduction of Pt^{2+} in β and L zeolites [3,14], while autoreduction of Fe^{3+} during calcination has also been reported by Jacobs [41]. The reduction of iron in presence of platinum appears to be more effective, and it therefore yields a larger ESR signal. The presence of reduced Fe^{2+} in close contact with Pt^{2+} may act as a "chemical anchor" for the latter and will retain a high dispersion of platinum after reduction [5]. This may be the origin of the better dispersion of bimetallic Pt–Fe/KL-2 zeolite than mono-metallic Pt/KL (Table 1).

3.4. Reduction of Pt^{2+} and Fe^{3+} ions

TPR spectra of mono-metallic 5% Pt/KL (a) and 0.3% Fe/KL (c), together with bimetallic 5% Pt-0.3% Fe/KL (b), all after the same calcination treatment, are shown in Fig. 5. Pt^{2+} ions in Pt/KL are reduced

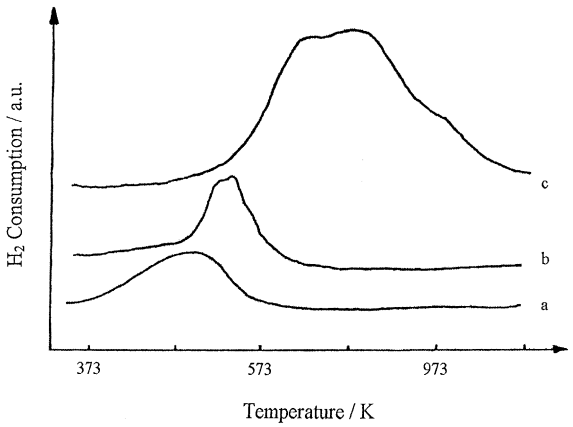

Fig. 5. TPR spectra of calcined samples: (a) 5% Pt/KL; (b) 5% Pt-0.3% Fe/KL; (c) 0.3% Fe/KL.

in a narrow temperature range with maximum near 493 K. Fe^{3+} ions in Fe/KL zeolite, on the contrary, are reduced at higher temperature (573–773 K). In the bimetallic zeolite, the reduction temperature (with maximum at about 543 K) is slightly higher than that of the mono-platinum supported zeolite but significantly smaller than that of Fe/KL. Fe^{3+} in the bimetallic sample could be reduced already at 473 K, about 100 K lower than in the absence of platinum. The relatively smaller area of the reduction peak, comparing bimetallic with mono-iron supported zeolite (Fig. 5), is due to the partial autoreduction of Fe^{3+} to Fe^{2+} during calcination, as discussed above.

The fact that only one TPR peak is observed in an intermediate temperature range, instead of two separate peaks (one for Pt at low and one for Fe at higher temperature), confirms the interaction of Pt and Fe oxide species and the formation of a Pt–Fe alloy. Similar phenomena were found in the alloy formation of Pt–Re/Al_2O_3 [42].

Figs. 6 and 7 show the room temperature ESR spectra of mono-iron and bimetallic samples reduced at different temperature. For 0.3% Fe/KL there is almost no difference in the signal intensity when the reduction temperature changes from 373 to 573 K (Fig. 6a–c). After reduction at higher temperature (673 K), the amplitude of the broad ESR signal at $g = 2.3$ increases greatly, becoming much broader and even covering the signal at lower magnetic field (Fig. 6d and e). As already discussed above, the large increase of this signal is due to the partial reduction of Fe^{3+} to Fe^{2+} or Fe^0.

It is interesting to find that reduction of bimetallic Pt–Fe/KL causes the same signal ($g = 2.3$) to increase greatly already at 573 K (Fig. 7b). For clarity, the intensities of the ESR signals as a function of reduction

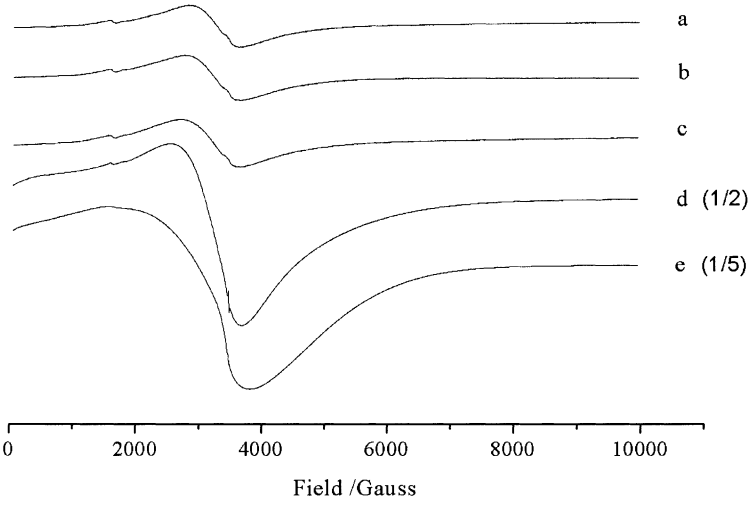

Fig. 6. Room temperature ESR spectra of 0.3%Fe/KL reduced at: (a) 373 K; (b) 473 K; (c) 573 K; (d) 673 K; (e) 773 K. The amplitudes of spectra (d) and (e) are scaled by a factor of 0.5 and 0.2, respectively.

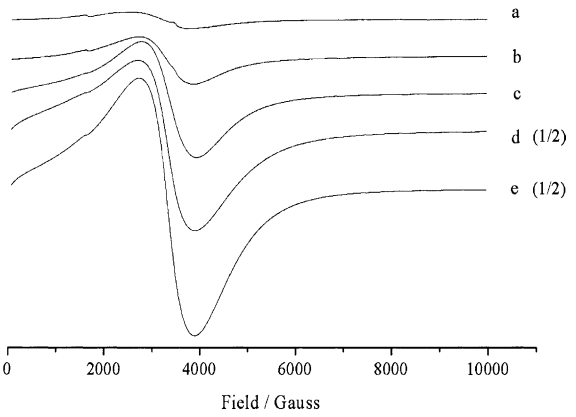

Fig. 7. Room temperature ESR spectra of 5% Pt-0.3% Fe/KL reduced at: (a) 373 K; (b) 473 K; (c) 573 K; (d) 673 K; (e) 773 K. The amplitudes of spectra (d) and (e) are scaled by a factor of 0.5.

temperature are shown in Fig. 8. Considering the nature of this increase in intensity it is clear that there is a nearly 100 K decrease of the reduction temperature of Fe^{3+} in presence of Pt, which is well consistent with TPR and confirms the interaction of Pt with Fe. The bimetallic Pt–Fe^{n+} clusters are more electrophilic (as shown already by CO-IR results in Table 1) which therefore weakens the strength of the S–Pt bond and causes the improved sulfur resistance.

The behavior of 1 wt.% Pt-0.3 wt.% Fe/KL (the Pt content of which is sufficiently close to that used in catalysis studies) is very similar to that of 5 wt.% Pt-0.3% Fe/KL and thus shows good correlation between catalysis and characterization. Fig. 8 also shows that the signal on plain KL zeolite keeps constant for different reduction temperatures, demonstrating that the Fe impurity does not distort the results.

ESR spectroscopy at lower temperature (150 and 4 K) on 5 and 1 wt.% Pt supported samples results in almost the same trend of increasing intensity of the $g = 2.3$ signal. The reproducibility of this phenomenon proves the usefulness of ESR for the characterization of this system.

Based on present studies it is still not possible to decide without doubt whether reduction of Fe^{3+} results in the formation of Fe^{2+} or metallic Fe^0 or metallic Pt-Fe alloy, and we do not know exactly the related magnetic properties. Mössbauer experiments are planned, SQUID magnetization measurements are in progress, and the results will be published in due course.

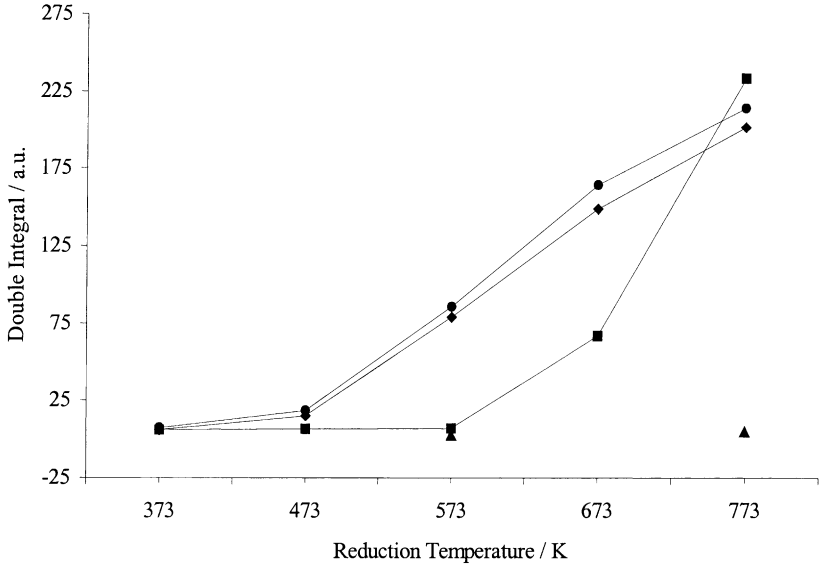

Fig. 8. The intensities of ESR signals as a function of reduction treatment temperature: (▲) KL; (■) 0.3% Fe/KL; (◆) 1% Pt-0.3% Fe/KL; (●) 5% Pt-0.3% Fe/KL.

4. Conclusions

The influence of Fe as a second metal component on a Pt/KL zeolite catalyst has been investigated. The characteristic difference between bimetallic and mono-metallic supported zeolites can be described as follows:

1. Co-impregnation of iron stabilizes the *cis*-platinum complexes in KL zeolite.
2. XPS results show that Pt^{2+} ions migrate onto inner sites of KL crystallites during calcination, leaving only a slight enrichment on the surface. In contrast, Fe^{3+} shows a very pronounced surface enrichment.
3. Partial autoreduction of Fe^{3+} occurs during calcination, as evidenced by the large increase of the ESR signal with a *g*-factor around 2.3. This process is facilitated by the presence of Pt.
4. Pt also "catalyzes" the reduction of Fe^{3+} in hydrogen, causing nearly 100 K decrease of the reduction temperature.
5. After reduction, the Pt particles are more electron deficient owing to the partial electron transfer from Pt to Fe^{n+} ions. As a consequence, the bimetallic Pt–Fe/KL zeolite shows a higher performance on both catalytic activity for *n*-hexane aromatization and sulfur resistance.

Acknowledgements

We are grateful to CU Chemie Uetikon AG in Switzerland for providing KL zeolite for our research, and we thank Prof. R. Stösser for useful discussions.

References

[1] J.A. Rabo, V. Schomaker, P.E. Picket, in: Proceedings of the International Congress on Catalysis, Vol. 2, 3rd Edition, North Holland, Amsterdam, 1965, p. 1264.
[2] W.M.H. Sachtler, Catal. Today 15 (1993) 419.
[3] J. Zheng, J.L. Dong, Q.H. Xu, Stud. Surf. Sci. Catal. 84 (1994) 1641.
[4] S. Ciccariello, A. Benedetti, F. Pinna, G. Strukul, W. Juszczyk, H. Brumberger, Phys. Chem. Chem. Phys. 1 (1999) 367.
[5] M.S. Tzou, B.K. Teo, W.M.H. Sachtler, J. Catal. 113 (1988) 220.
[6] Y. Huang, W.M.H. Sachtler, J. Catal. 188 (1999) 215.
[7] J. Jia, J. Shen, L. Lin, Z. Xu, T. Zhang, D. Liang, J. Mol. Catal. A: Chem. 138 (1999) 177.
[8] L. Xu, G. Lei, W.M.H. Sachtler, R. Cortright, J.A. Dumesic, J. Phys. Chem. 97 (1993) 11517.
[9] V. Schünemann, H. Treviño, W.M.H. Sachtler, K. Fogash, J.A. Dumesic, J. Phys. Chem. 99 (1995) 1317.
[10] V. Schünemann, H. Treviño, G.D. Lei, D.C. Tomczak, W.M.H. Sachtler, K. Fogash, J.A. Dumesic, J. Catal. 153 (1995) 144.
[11] T.R. Hughes, W.C. Buss, P.W. Tamm, R.L. Jacobson, Stud. Surf. Sci. Catal. 28 (1986) 725.
[12] E.G. Derouane, D.J. Vanderveken, Appl. Catal. 45 (1988) L15.
[13] S.T. Tauster, J.J. Steger, J. Catal. 125 (1990) 387.
[14] J. Zheng, J.L. Dong, Q.H. Xu, C. Hu, Catal. Lett. 37 (1996) 25.
[15] J.R. Bernard, in: Proceedings of the 5th International Conference on Zeolites, Heyden, London, 1980, p. 686.
[16] P.W. Tamm, D.H. Mohr, C.R. Wilson, Stud. Surf. Sci. Catal. 38 (1987) 335.
[17] M. Vaarkamp, J.T. Miller, F.S. Modica, G.S. Lane, D.C. Koningsberger, J. Catal. 138 (1992) 675.
[18] G.B. McVicker, J.L. Kao, J.J. Ziemiak, W.E. Gates, J.L. Robbins, M.M.J. Treacy, S.B. Rice, T.H. Vanderspurt, V.R. Cross, A.K. Ghosh, J. Catal. 139 (1993) 48.
[19] T. Fukunaga, V. Ponec, J. Catal. 157 (1995) 550.
[20] M. Guenin, M. Breysse, R. Frety, K. Tifouti, P. Marecot, J. Barbier, J. Catal. 105 (1987) 144.
[21] W.M.H. Sachtler, A.Y. Starheev, Catal. Today 12 (1992) 283.
[22] G. Connell, J.A. Dumesic, J. Catal. 101 (1986) 103.
[23] J.K. Lee, H.K. Rhee, J. Catal. 177 (1998) 208.
[24] G.N. Sauvion, I.M. Akelay, F. Guilleux, J.F. Tempere, D. Delafosse, J. Chim. Phys. 80 (1983) 769.
[25] S.V. Gagarin, Structure and Reactivity of Modified Zeolite, Elsevier, Amsterdam, 1984, p. 345.
[26] G.C. Xu, J.Y. Wang, ShiYou XueBao (ShiYou JiaGong) 8 (1992) 29.
[27] S. Sirasanki, React. Kinet. Catal. Lett. 136 (1988) 173.
[28] J. Zheng, J.L. Dong, Q.H. Xu, Appl. Catal. 126 (1995) 141.
[29] J.L. Dong, J.H. Zhu, Q.H. Xu, Appl. Catal. 112 (1994) 105.
[30] C. Besoukhanova, J. Guidot, D. Barthomeuf, J. Chem. Soc., Faraday Trans. 1 77 (1991) 1595.
[31] T. Rades, V.Yu. Borovkov, V.B. Kazansky, M. Polisset-Thfoin, J. Fraissard, J. Phys. Chem. 100 (1996) 16238.
[32] H. Bischoff, N.I. Jaeger, G. Schulz-Ekloff, J. Catal. 80 (1993) 95.
[33] J. Zheng, J.L. Dong, Q.H. Xu, Chin. J. Mol. Catal. 12 (1998) 113.
[34] Y. Sakamoto, K. Higuchi, N. Takahashi, K. Yokota, H. Doi, M. Sugiura, Appl. Catal. B: Environ. 23 (1999) 159.
[35] C.W. Bartholomew, M. Boudart, J. Catal. 29 (1973) 278.
[36] P. Ratnasami, R. Kumar, Catal. Today 9 (1991) 328.
[37] D. Goldfarb, M. Berbardo, K.G. Strohmaier, D.E.W. Vaughan, H. Thomann, J. Am. Chem. Soc. 116 (1994) 6344.
[38] G. Scholz, R. Stösser, T. Grande, S. Aasland, Ber. Bunsenges. Phys. Chem. 101 (1997) 1291.
[39] K.M. Sancier, S.H. Inami, J. Catal. 11 (1968) 135.
[40] L.M. Kustov, V.B. Kazansky, P. Ratnasamy, Zeolites 7 (1987) 79.
[41] P.A. Jacobs, Stud. Surf. Sci. Catal. 29 (1986) 357.
[42] G. Fröhlich, W.M.H. Sachtler, J. Chem. Soc., Faraday Trans. 1 94 (1998) 1339.